Journal of Applied Electrochemistry **32**: 513–520, 2002.

Preparation and electrochemical characterization of $Ti/Ru_xMn_{1-x}O_2$ electrodes

J.L. FERNÁNDEZ, M.R. GENNERO DE CHIALVO and A.C. CHIALVO*
Programa de Electroquímica Aplicada e Ingeniería Electroquímica (PRELINE), Facultad de Ingeniería Química, Universidad Nacional del Litoral, Santiago del Estero 2829, 3000 Santa Fe, Argentina
*(*author for correspondence, fax: +54 342 457 1162, e-mail: achialvo@fiqus.unl.edu.ar)*

Received 4 September 2001; accepted in revised form 2 January 2002

Key words: chlorine evolution, DSA®, oxygen evolution, ruthenium–manganese mixed oxides

Abstract

DSA® type electrodes of ruthenium–manganese mixed oxides ($30 \leqslant$ at % Ru < 100) supported on titanium were prepared by the spray-pyrolysis technique, using $Ru(NO)(OH)_x(NO_3)_{3-x}$ and $Mn(NO_3)_2$ as precursors. Electrodes were characterized by SEM, XRD and cyclic voltammetry. Their behaviour as anode for the chlorine and oxygen evolution reactions was also evaluated by polarization curves. The stability of the mixed oxides was determined through accelerated tests of service life. It has been verified that the best performance on the apparent electrocatalytic activity of both reactions as well as on stability is achieved at a composition of about 70% Ru.

1. Introduction

Ruthenium dioxide is the main component of DSA® electrodes, extensively used as anodes in several electrochemical industrial processes [1], especially in chlor-alkali cells [2]. These supported materials contain Ru(IV) partially substituted by other cations which form oxides that are isomorphous with RuO_2, mainly Ti(IV), Ir(IV) and Sn(IV), in order to improve the stability and selectivity of the electrodes [3, 4].

Among these cations, several authors [5–11] have considered that Mn(IV) is appropriate to partially substitute Ru(IV) in the oxide. In their studies they used mostly mixtures of $RuCl_3$ and $Mn(NO_3)_2$ as precursors of the oxides, preparing the supported layers by the dipping technique. These electrodes were evaluated for processes like oxygen (OER) [5–7] and chlorine (ClER) [7–9] electrode reactions, as well as chlorate production from chloride [10]. With the exception of the work by Iwakura et al., who made a preliminary structural analysis of the films [11], these studies do not contain any reference to the chemical nature or the morphological characteristics of the electroactive material. Nevertheless, it is believed [7, 11] that the main reason for the favourable effect of the manganese addition into the ruthenium oxide is the formation of a solid solution between both cations. This would take place because the decomposition products of $RuCl_3$ and $Mn(NO_3)_2$ at the preparation temperature (450 °C) are RuO_2 and β-MnO_2, respectively, which are isomorphic and have similar cell dimensions [4]. However, the use of $RuCl_3$ as precursor could be inappropriate, since the decomposition of Mn(II) in the presence of chloride ions could lead to a mixture of different oxides [12, 13], inhibiting the desired substitution.

The present work deals with the preparation of mixed oxides of ruthenium and manganese supported on titanium by the spray-pyrolysis technique. Special emphasis was put in obtaining a solid solution as the main electroactive material, so that the respective nitrates were used as starting precursors. It was also intended to obtain structurally and morphologically well-characterized films. This study was oriented to the evaluation of the behaviour of these electrodes as anodes at high overpotentials, such as those needed for the OER and ClER reactions. The characterization was carried out by the analysis of the polarization curves for a wide range of overpotentials, cyclic voltammetry and accelerated service life tests.

2. Experimental details

2.1. *Preparation of the electrodes*

Ruthenium and manganese mixed oxides supported on titanium were prepared through a variation of the spray-pyrolysis technique previously developed [14]. Precursor solutions with $0.1 \leqslant f_{Ru} \leqslant 1$, being f_{Ru} the ruthenium atomic fraction in the precursor, were prepared mixing appropriate volumes of solutions of $Ru(NO)(OH)_x(NO_3)_{3-x}$ (Aldrich) and $Mn(NO_3)_2$ (Merck) in 0.1 M HNO_3, in order to obtain a 0.16 M cationic concentration solution. The substrates were titanium wires 99.7%

(Aldrich) of 0.8 mm diameter and 4 cm length. They were subjected to a mechanical polishing with emery paper and a chemical etching with a HNO_3–HF–H_2O 1:1:10 solution during 5 s. They were then rinsed with triply distilled water and dried at 50 °C. Each substrate wire was located in the spray-pyrolysis device and heated by the Joule effect at 2 W cm^{-1}. The droplets of the precursor solution were generated through an ultrasonic atomizer and transported to the substrate surface by airflow at a rate of 40 cm s^{-1}. The spray-pyrolysis was applied for 4 min. To ensure complete decomposition, as well as uniformity in the film concentration, a thermal treatment was applied at 370 °C for 48 h.

Taking into account that β-MnO_2 could be segregated during the formation of the mixed oxide of Ru and Mn and that it is unstable in acidic NaCl solutions [15], electrodes were immersed in a 6 M HCl solution for 48 h to eliminate this phase. It should be taken into account that these electrodes, named Ti/$Ru_xMn_{1-x}O_2$, are different from those described in the literature [5–11], as they were prepared starting from the nitrate salts as precursors and the final chemical treatment produces a film with different structural and morphological properties.

2.2. *Structural and morphological characterization of the electrodes*

The morphological characterization of the oxide electrodes was carried out by scanning electron microscopy on a Jeol JSM-35C microscope, while the structural analysis was made by X-ray diffraction of the powder obtained by peeling off the films, using a powder diffractometer Shimadzu XD-D1 with CuK_α radiation.

2.3. *Electrochemical characterization*

Electrochemical measurements were carried out in a conventional three-electrode Pyrex glass cell. Ru_x-$Mn_{1-x}O_2$ films supported on titanium prepared as described in the previous section were used as working electrodes, while a platinum wire of large area was used as counterelectrode. Electrolytic solutions were prepared using analytical grade reagents and triply distilled water. All runs were carried out at 30 ± 0.1 °C.

Voltammetric experiments were run in NaCl – HCl (C_{Cl^-} = *4* M, pH 1.1) and also in 0.5 M H_2SO_4, using a potentiostat/galvanostat Radiometer PGP201 monitored by the software VoltaLab™ 21. The reference electrode used was saturated calomel (SCE).

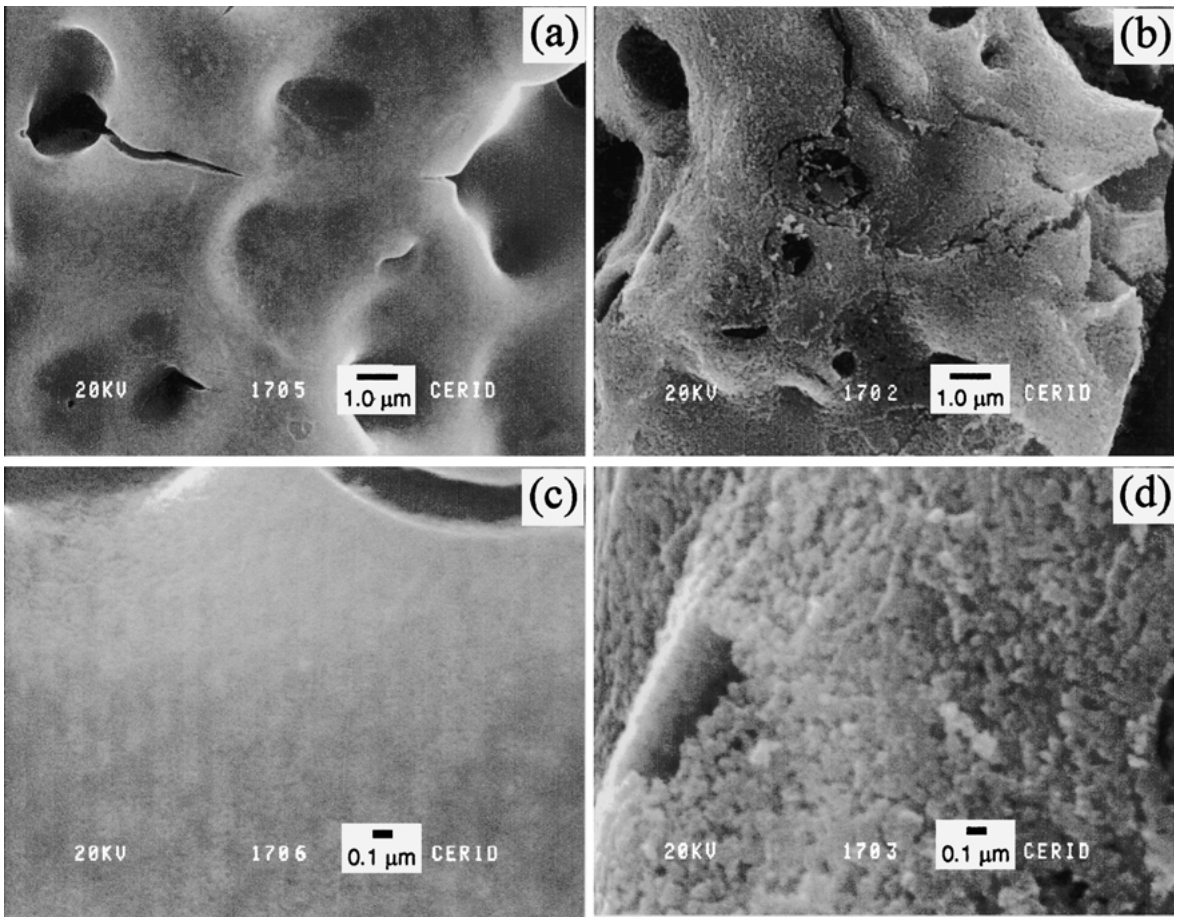

Fig. 1. SEM micrographs of a Ru–Mn mixed oxide electrode ($f_{Ru} = 0.4$) prepared by spray-pyrolysis. (a and c) before; (b and d) after etching in HCl. Magnification: 9400 × (a and b), 40 000 × (c and d).

The apparent electrocatalytic activity of the electrodes, relative to the geometric area, for the ClER was evaluated in NaCl – HCl ($C_{Cl^-} = 4$ M) solutions, saturated with chlorine (1 atm) at different pH values. Polarization curves were obtained through the application of slow potentiodynamic sweeps (10^{-4} V s^{-1}) starting from 1.24 V vs SCE and up to 1.04 V.

The behaviour of the $Ti/Ru_xMn_{1-x}O_2$ electrodes for the OER was also studied in 0.5 M H_2SO_4 solution saturated with oxygen (1 atm), through polarization curves obtained in the same way as those for the ClER, from 1.39 V and up to 1.08 V vs SCE.

The electrochemical stability of these electrodes was also determined through accelerated service life tests in 0.5 M H_2SO_4 at an apparent current density of 1 A cm^{-2} [16].

3. Results

3.1. *Characterization of the mixed oxides films*

The morphology of the mixed oxides films prepared by spray-pyrolysis is similar to that corresponding to a RuO_2 film obtained by the same technique from $RuCl_3$ solutions [14]. Oxide films with very good covering properties were obtained in the whole range of manganese compositions. However, those corresponding to low ruthenium contents ($f_{Ru} \leqslant 0.5$) are strongly damaged by chemical etching in HCl, because in this case the amount of β-MnO_2 is important. The effect of such etching on the micro morphology of the oxide layers can be observed in the micrographs of Figure 1.

X-ray diffraction spectra of some of the obtained mixed oxides are shown in Figure 2 as prepared and in Figure 3 after the chemical etching. Peaks corresponding to the rutile phase of the mixed oxide $Ru_xMn_{1-x}O_2$ are observed in both cases, located at angle values intermediate to those of pure RuO_2 and β-MnO_2 [17, 18]. The signals corresponding to β-MnO_2 can be appreciated when $f_{Ru} < 0.7$ only on the spectra of the nontreated oxides. This evidence demonstrates the effectiveness of the dissolution carried out during the etching process. No peaks could be attributed to α-Mn_2O_3, coming from the decomposition of β-MnO_2 [19], as well as those corresponding to phases containing titanium from the substrate.

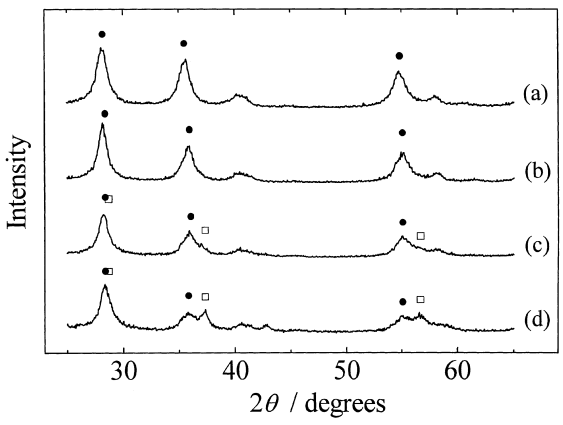

Fig. 2. XRD spectra of Ru–Mn mixed oxides prepared by thermal decomposition at 370 °C. f_{Ru}: 0.9 (a), 0.7 (b), 0.5 (c), 0.3 (d). Points: main diffraction peaks of $Ru_xMn_{1-x}O_2$ (●) and β-MnO_2 (□).

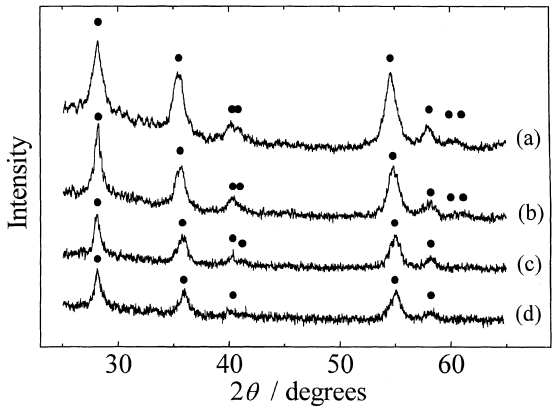

Fig. 3. XRD spectra of Ru–Mn mixed oxide films prepared by spray-pyrolysis, etched in HCl. f_{Ru}: 0.9 (a), 0.7 (b), 0.5 (c), 0.3 (d). Points: diffraction peaks of $Ru_xMn_{1-x}O_2$ (●).

The potentiodynamic responses are illustrated in Figures 4 and 5, corresponding to NaCl and H_2SO_4 solutions, respectively. They are different from that of RuO_2 electrodes [20–22]. The main difference is the enhancement of the process that takes place at ~0.4 V vs SCE, being more evident when $0.6 \leqslant f_{Ru} \leqslant 0.8$. There is also a marked difference in the cathodic region of the voltammograms when f_{Ru} is changed from 0.7 to 0.6, with a decrease in the voltammetric charge as the ruthenium content decreases.

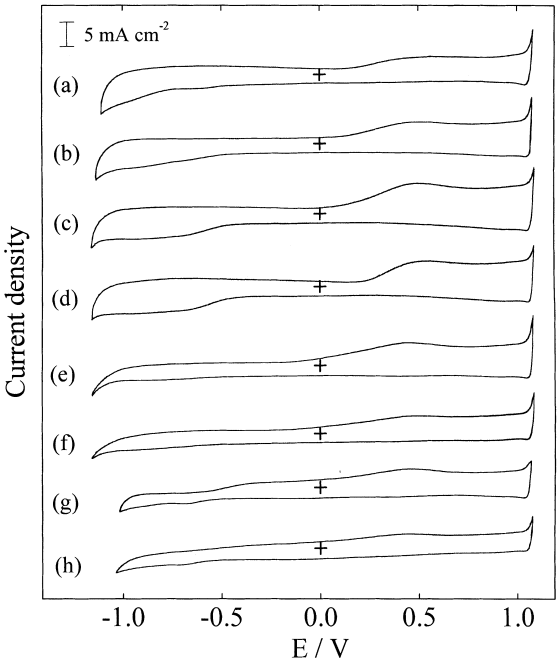

Fig. 4. Voltammograms of $Ti/Ru_xMn_{1-x}O_2$ electrodes. f_{Ru}: 1 (a), 0.9 (b), 0.8 (c), 0.7 (d), 0.6 (e), 0.5 (f), 0.4 (g), 0.3 (h). Electrolyte solution: NaCl–HCl, $C_{Cl^-} = 4$ M, pH 1.2. $T = 30$ °C. Sweep rate 0.1 V s^{-1}. Reference electrode: SCE.

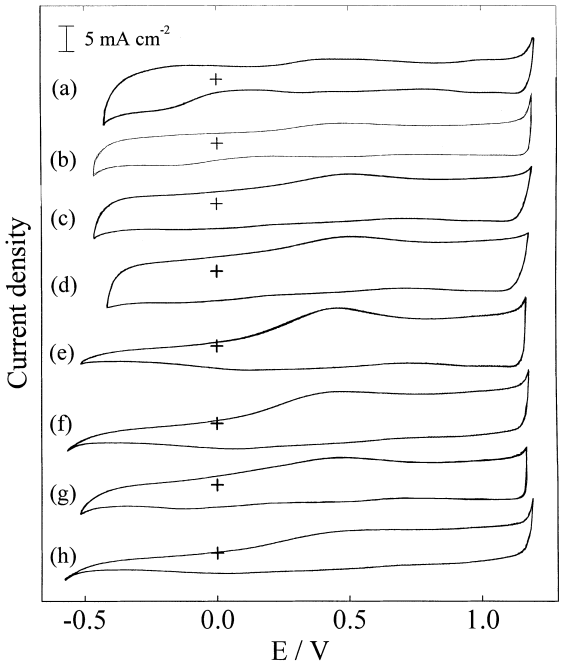

Fig. 5. Voltammograms of $Ti/Ru_xMn_{1-x}O_2$ electrodes. f_{Ru}: 1 (a), 0.9 (b), 0.8 (c), 0.7 (d), 0.6 (e), 0.5 (f), 0.4 (g), 0.3 (h). Electrolyte solution: H_2SO_4 0.5 M. $T = 30$ °C. Sweep rate = 0.1 V s^{-1}. Reference electrode: SCE.

3.2. *Apparent electrocatalytic activity for the ClER*

The rest potential of the $Ti/Ru_xMn_{1-x}O_2$ electrodes in NaCl–HCl solutions saturated with chlorine gas reaches a steady state value very rapidly, corresponding to the equilibrium potential of the chlorine electrode reaction.

The polarization curves obtained in this solution are shown in Figure 6. They were determined at three different pH values, which were measured after saturation with chlorine. A set of results (Figure 6(a)) corresponds to pH 2.1, where the hydrolysis of chlorine to hypochlorite is significant [23] and the oxygen evolution can be an important secondary reaction [24, 25], as well as the corrosion of RuO_2 to $RuO_{4(g)}$ at high overpotentials [26, 27]. Figure 6(b) illustrates the polarization curves corresponding to pH 1.0, where the ClER is the main electrode reaction [25]. Finally, those corresponding to pH 0.1 are shown in Figure 6(c), where the acidity of the solution produces oxidation of the ruthenium oxide to soluble species [26].

The values of the apparent current density j^{ap} at different potentials were obtained from the polarization curves of Figure 6 for each of the electrodes with different oxide composition. These values were plotted against f_{Ru} and the corresponding dependences are shown in Figure 7. For the range of compositions between pure RuO_2 and $f_{Ru} \simeq 0.8$, an increase in the j^{ap} values are observed for the more acidic solutions. j^{ap} then decreases as the amount of manganese in the mixed oxide increases. This behaviour is not observed in the solution of pH 2.1, where the j^{ap} values of the mixed oxide are always less than those corresponding to RuO_2.

3.3. *Apparent electrocatalytic activity for the OER*

The polarization curves obtained for the $Ti/Ru_xMn_{1-x}O_2$ electrodes in 0.5 M H_2SO_4 solution saturated with oxygen gas are illustrated in Figure 8. The polarization curves corresponding to the ClER in NaCl

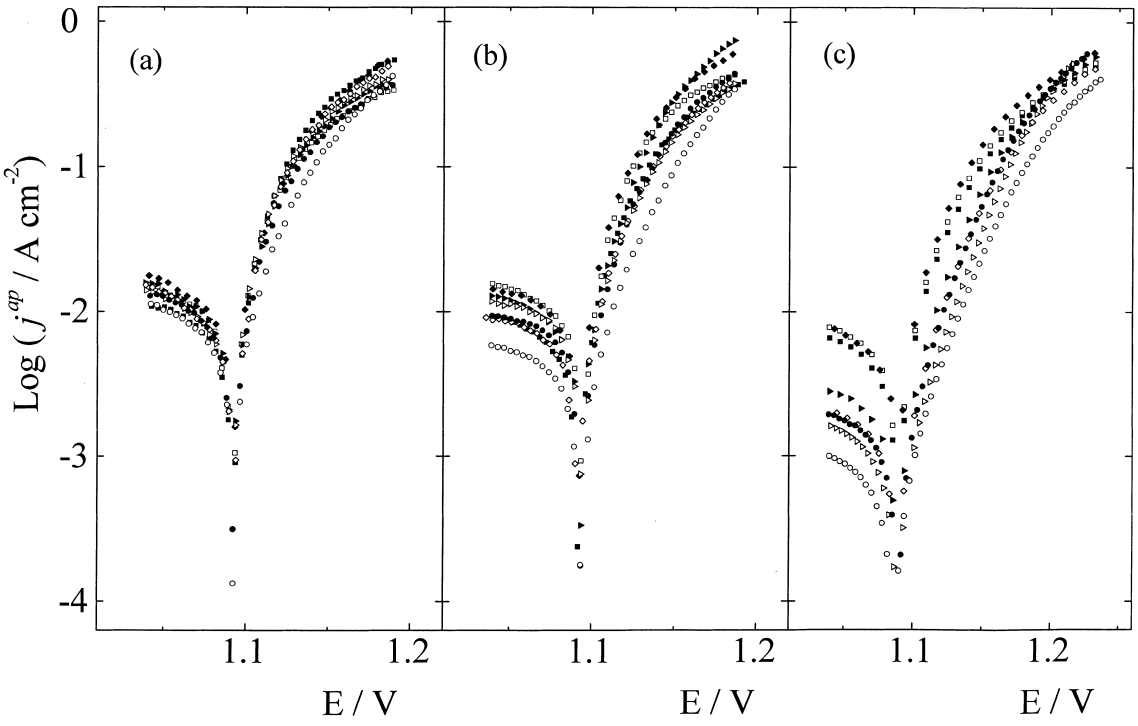

Fig. 6. Polarization curves of $Ti/Ru_xMn_{1-x}O_2$ electrodes. f_{Ru}: 1 (■); 0.9 (□); 0.8 (◆); 0.7 (▲); 0.6 (△); 0.5 (◇); 0.4 (●); 0.3 (○). Electrolyte solution: NaCl–HCl saturated with chlorine (1 atm), $C_{Cl^-} = 4$ M, pH 2.1 (a), 1.0 (b), 0.1 (c). $T = 30$ °C. Reference electrode: SCE.

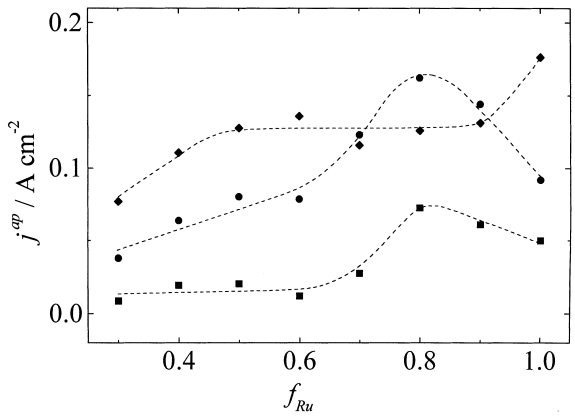

Fig. 7. Dependences j^{ap} vs f_{Ru} obtained on $Ti/Ru_xMn_{1-x}O_2$ electrodes. Electrolyte solution: NaCl–HCl saturated with chlorine (1 atm), $C_{Cl^-} = 4$ M, pH 2.1 (◆), 1.0 (●), 0.1 (■). E vs SCE: 1.13 V.

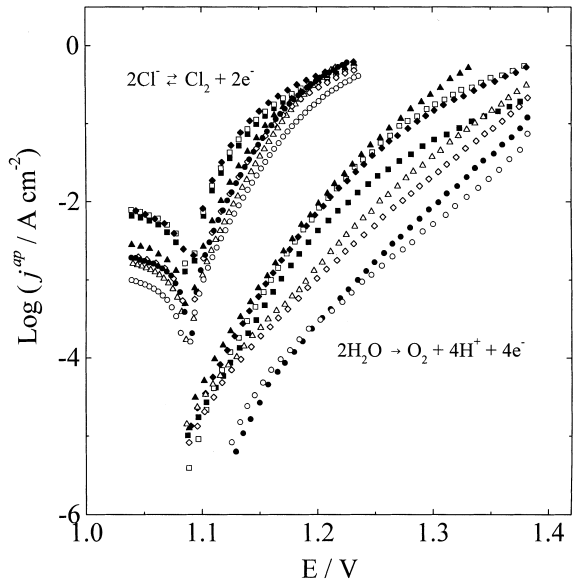

Fig. 8. Polarization curves of $Ti/Ru_xMn_{1-x}O_2$ electrodes. f_{Ru}: 1 (■); 0.9 (□); 0.8 (◆); 0.7 (▲); 0.6 (△); 0.5 (◇); 0.4 (●); 0.3 (○). Electrolyte solution: H_2SO_4 0.5 M saturated with oxygen (1 atm). $T = 30$ °C. Reference electrode: SCE. Polarization curves of Fig. 6(c) are included as comparison.

and pH 0.1 are also included in Figure 8 for the sake of comparison. It can be clearly appreciated that the currents for the OER are more than two orders of magnitude less than those corresponding to the ClER at the same overpotential values, which is in agreement with previous reports [24, 25].

The values of j^{ap} at certain potentials were obtained for each electrode in the same way as for the ClER. The corresponding dependences j^{ap} vs f_{Ru} are illustrated in Figure 9. j^{ap} values increase with increase in the manganese content in the more acidic solutions, in agreement with previous results [10]. However, in this case j^{ap} passes through a maximum at $f_{Ru} \simeq 0.7$ and then decreases up to a value slightly less than that obtained on RuO_2.

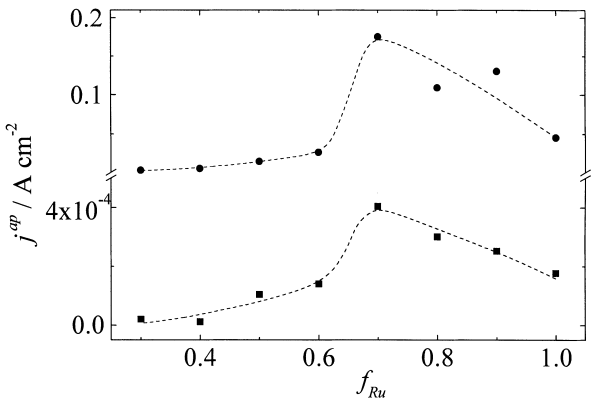

Fig. 9. Dependences j^{ap} vs f_{Ru} obtained on $Ti/Ru_xMn_{1-x}O_2$ electrodes. Electrolyte solution: H_2SO_4 0.5 M saturated with oxygen (1 atm). E vs SCE: 1.14 V (■), 1.29 V (●).

3.4. *Stability*

$Ti/Ru_xMn_{1-x}O_2$ electrodes were subjected to an apparent current density of 1 A cm^{-2} in 0.5 M H_2SO_4 solution in order to analyse their stability. The potential against time dependences are shown in Figure 10. From these transient plots and following the procedure described by Loučka [16], the corresponding time-to-failure (τ) was obtained; these are illustrated as a function of f_{Ru} in Figure 11.

The values of τ obtained in electrodes prepared in an identical way but without etching in HCl are also included in Figure 11. It can be observed that for $f_{Ru} \geqslant 0.7$ there is no difference between the behaviour of both treated and un-treated electrodes. However, for $f_{Ru} < 0.7$, the process of dissolution of β-MnO_2 produces a marked decrease in the time-to-failure of the electrodes.

4. Discussion

It has been considered that the study of DSA®-type electrodes based in mixed oxides of ruthenium and

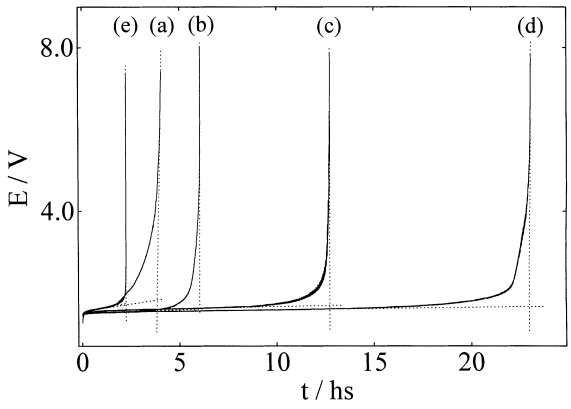

Fig. 10. Dependences potential against time obtained on $Ti/Ru_xMn_{1-x}O_2$ electrodes during the accelerated tests of service life. f_{Ru}: 1 (a), 0.9 (b); 0.8 (c); 0.7 (d), 0.6 (e). H_2SO_4 0.5 M, $T = 25$ °C, $j^{ap} = 1$ A cm^{-2}. Reference electrode: SCE.

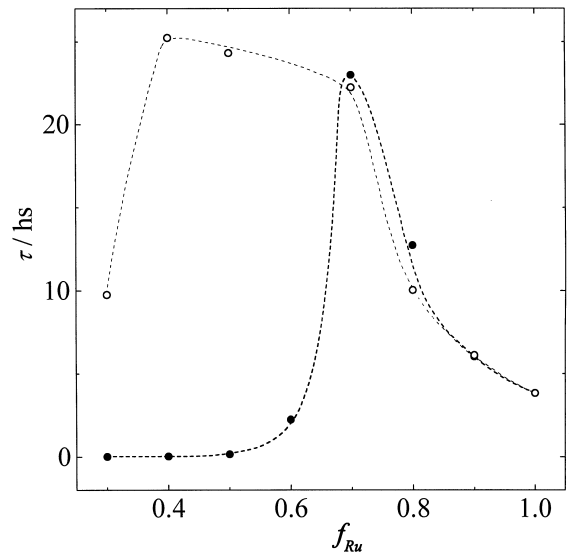

Fig. 11. Time-to-failure (τ) vs f_{Ru}. Ti/$Ru_xMn_{1-x}O_2$ electrodes (●). Ru–Mn mixed oxides without etching in HCl (○).

manganese should be of interest due to their potential use as anodes in several electrochemical processes such as the chlorine and oxygen evolution reactions.

Electrodes were prepared by a modification of the spray-pyrolysis technique, developed previously for obtaining cylindrical electrodes of Ti/RuO_2, from the thermal decomposition of $RuCl_3$ solutions [14]. Therefore, the different variables that influence the preparation of these mixed oxides by thermal decomposition of the precursor solution containing both cations were optimised. On the basis of a previous study of the decomposition process of different ruthenium salts mixed with $Mn(NO_3)_2$, the convenience of the use of ruthenium nitrate was determined. Therefore, the mixed precursor used consisted of a mixture of Ru(NO)-$(OH)_x(NO_3)_{3-x}$ and $Mn(NO_3)_2$ in dilute HNO_3.

The characterization of the oxide films by X-ray diffraction indicates that they consisted of the same material obtained as a powder through a process of drying and decomposition of the precursor solutions at 370 °C. The main component is a mixed oxide with a rutile structure of a stoichiometry $Ru_xMn_{1-x}O_2$, with $0.6 < x < 1$ [13]. The β-MnO_2, which is present when $f_{Ru} < 0.7$, can be eliminated by etching in a concentrated HCl solution [15]. Therefore, this treatment was applied to the electrodes in order to have the mixed oxide as the unique component of the films. The complete removal of β-MnO_2 from the film was achieved, yet at lower compositions of ruthenium.

The SEM observations at high magnification (Figure 1) indicates that the selective dissolution of the β-MnO_2 phase reveals superficially mixed oxide crystallites, with sizes less than 100 nm, producing a remarkable increase in the micro roughness of the film. It should be noticed that the mechanical resistance of the oxide films is good, but the chemical etching reduces this property in the electrodes with high manganese content, producing complete detachment of the film when $f_{Ru} < 0.3$. It is also important to mention that this treatment was made in order to obtain a purer material, so as to ensure that $Ru_xMn_{1-x}O_2$ is mainly responsible for the observed electrochemical response. Dissolution in the electrolyte solutions is also avoided, particularly in those containing chloride ions.

The voltammetric responses of the Ti/$Ru_xMn_{1-x}O_2$ electrodes in both NaCl and H_2SO_4 solutions show slight differences with respect to those of the Ti/RuO_2 electrodes, which should reveal interactions between manganese and ruthenium inside the rutile lattice. The voltammograms recorded in sulfuric acid solution show some differences compared to those reported by Visvanathan et al. [6] obtained on mixed oxide electrodes prepared from ruthenium chloride and manganese nitrate, which indicates the different nature of the films under comparison. Well-defined reversible peaks are observed in these voltammograms between −0.4 and 0.4 V vs SCE, whereas in the Ti/$Ru_xMn_{1-x}O_2$ response there is a unique peak in this potential region.

For the chlorine evolution reaction, high values of the apparent current density (up to 0.8 A cm^{-2}) were registered at relatively low overpotentials ($\eta \leqslant 0.15$ V). This value is in the range of the higher values usually published (from 0.1 to 1 A cm^{-2}) for electrodes based on RuO_2 and prepared through thermal decomposition [27–32]. The adverse effect of the increase in acidity is also evident, especially at low overpotentials, as previously reported [30].

The polarization curves corresponding to the ClER are characterized by the absence of a clear Tafelian region. However, a pseudo-Tafelian domain [33] with a slope of ~40 mV dec^{-1} can be identified in the curves recorded at lower pH, similar to those reported for RuO_2 and RuO_2–TiO_2 electrodes in the same media [30–32]. From the comparison of the responses of all the Ti/$Ru_xMn_{1-x}O_2$ electrodes, a group characterized by a f_{Ru} between 0.7 and 1.0 is evident. These electrodes have greater activity than the others over most of the potential range. It was determined from the observation of the dependences j^{ap} vs f_{Ru} at different potential values that the apparent electrocatalytic activity in the more acidic solutions increases with the manganese content, passing through a maximum at $f_{Ru} \simeq 0.7$–0.8 and then decreasing with further addition of this cation. This tendency is not fulfilled for the less acidic solution, where the influence of the secondary reactions is important, and therefore a decrease in j^{ap} is verified when manganese composition increases. Interesting features have been found in the behaviour of the Ti/$Ru_xMn_{1-x}O_2$ electrodes for the OER. The response of the Ti/RuO_2 electrode is similar to that previously reported [34–36], while the electrodes with $f_{Ru} \geqslant 0.7$ are significantly more active than that without manganese. The polarization curves have only one pseudo-Tafelian region with a slope of ~40 mV dec^{-1}. These results emphasise the positive effect of the addition of manganese to the rutile-type oxide when it is used as anode. For the electrodes with greater manganese content

($f_{Ru} < 0.7$), a marked decrease in the electrocatalytic activity was found. In this case the polarization curves show pseudo-Tafelian regions with slopes ranging between 60 and 80 mV dec^{-1}.

From accelerated life tests carried out on the $Ti/Ru_xMn_{1-x}O_2$ electrodes, it has been determined that the stability increases with the amount of manganese in the oxide. The time-to-failure increases almost five times with respect to that of the Ti/RuO_2 electrode. The main cause of this behaviour, as with those of ruthenium dioxide electrodes partially substituted by titanium [37], iridium [38] and tin [11, 28, 39], is the greater resistance of these materials to the anodic oxidation/dissolution. When the electrodes are etched in HCl before use, the stability reaches a maximum at a composition of approximately 30% manganese. For greater compositions ($f_{Ru} < 0.7$), stability decreases sharply. Nevertheless, this behaviour does not occur for electrodes not etched in HCl. In this case the increase in stability continues up to 60% manganese, which is in agreement with previous results [6, 11]. Therefore, the loss of stability at lower manganese contents is likely due to a decrease in the mechanical resistance of the mixed oxide films, originating in the selective dissolution of one of the phases during etching.

A complete analysis of the results obtained in the present work demonstrates that there is a breaking point in the behaviour of the mixed oxide electrodes when the ruthenium atomic fraction in the precursor solution is below 0.7. There are differences in the voltammetric responses and also in the polarization curves. The increases in the electrocatalytic activity and stability are also interrupted when $f_{Ru} < 0.7$.

On the basis of structural knowledge of these oxides, it can be asserted that for manganese contents greater than 30%, a separate β-MnO_2 phase is formed. When this phase is dissolved by etching in HCl weakness in the film is produced, which increases with β-MnO_2 content, the bare substrate being exposed in certain regions of the electrode surface. The mechanical stability of the film decreases sharply as does the time-to-failure of the electrode. Furthermore, the existence of titanium oxide in the electrode surface produces a decrease in apparent electrocatalytic activity, modifying both steady and dynamic current vs. potential responses. On the other hand, chemical etching does not affect electrodes with $f_{Ru} \geqslant 0.7$, as in this case the amount of β-MnO_2 is negligible.

5. Conclusions

The results suggest that manganese is an appropriate additive for electrodes based in RuO_2. When the films are prepared by thermal decomposition of the corresponding nitrates of both cations, a solid solution of rutile structure of stoichiometry $Ru_xMn_{1-x}O_2$ is obtained, which has a good performance as anode for reactions such as ClER and OER. Thus, an increase in the apparent electrocatalytic activity for both reactions, as well as in the anodic stability, is obtained when $0.7 \leqslant x \leqslant 0.9$. Below this composition, manganese forms a separate β-MnO_2 phase, which, in spite of being eliminated by chemical etching, produces a deterioration of the electrode properties.

Acknowledgement

The financial support of Consejo Nacional de Investigaciones Científicas y Técnicas (CONICET), Agencia Nacional de Promoción Científica y Tecnológica (ANPCYT) and Universidad Nacional del Litoral (UNL) is gratefully acknowledged.

References

1. S. Trasatti, *Electrochim. Acta* **45** (2000) 2377.
2. D.L. Caldwell, *in* J.O. Bockris, B.E. Conway, E. Yeager and R.E. White (Eds), 'Comprehensive Treatise of Electrochemistry', Vol. 2, (Plenum, New York, 1981), Chapter 2, p. 105.
3. S. Trasatti and G. Lodi, *in* S. Trasatti (Ed.), 'Electrodes of Conductive Metallic Oxides' Part A, (Elsevier, Amsterdam, 1980) Chapter 7, p. 301.
4. S. Trasatti, *in* J. Lipkowsky and P. Ross (Eds), 'Electrochemistry of Novel Materials' (VCH, New York, 1994), Chapter 5, p. 207.
5. D. Cipris and D. Pouli, *J. Electroanal. Chem.* **73** (1976) 125.
6. J. Prabhakar Rethinaraj, S.C. Chockalingam, S. Kulandaisamy and S. Visvanathan, *Bull. Electrochem.* **4** (1988) 969.
7. M. Morita, C. Iwakura and H. Tamura, *Electrochim. Acta* **23** (1978) 331.
8. M. Morita, C. Iwakura and H. Tamura, *Electrochim. Acta* **24** (1979) 639.
9. M. Morita, C. Iwakura and H. Tamura, *Denki Kagaku* **48** (1980) 12.
10. L.M. Elina, V.M. Gitneva and V.I. Bystrov, *Élektrokhimiya* **11** (1975) 1279.
11. Y. Kato, S. Nakamatsu, N. Furukawa and C. Iwakura, *Chem. Express* **7** (1992) 173.
12. G. Buisson, *J. Solid State Chem.* **19** (1976) 175.
13. J.L. Fernández, M.R. Gennero de Chialvo and A.C. Chialvo, *in* E.W. Brooman, C.M. Doyle, Ch. Comninellis and J. Winnick (Eds), 'Energy and Electrochemical Processes for a Cleaner Environment' PV 2001-23, The Electrochemical Society Proceedings Series, Pennington, NJ (2001), p. 508.
14. J.L. Fernández, M.R. Gennero de Chialvo and A.C. Chialvo, *J. Appl. Electrochem.* **27** (1997) 1323.
15. P. Pascal, 'Noveau Traité de Chimie Minérale', Vol. XVI (Masson et Cie, Paris,1960) p. 78.
16. T. Loučka, *J. Appl. Electrochem.* **11** (1981) 143.
17. JCPDS X-ray Powder Diffraction Files, 40-1290.
18. JCPDS X-ray Powder Diffraction Files, 24-735.
19. A.A. Abdul Azim, G.A. Kolta and M.H. Askar, *Electrochim. Acta* **17** (1972) 291.
20. T. Hepel, F.H. Pollak and W.E. O'Grady, *J. Electrochem. Soc.* **131** (1984) 2094; **133** (1986) 69.
21. K. Doblhofer, M. Metikoš, Z. Ogumi and H. Gerischer, *Ber. Bunsenges. Phys. Chem.* **82** (1978) 1046.
22. L.D. Burke and J.F. O'Neill, *J. Electroanal. Chem.* **101** (1979) 341.
23. Z. Nagy, *J. Electrochem. Soc.* **124** (1977) 91.
24. T. Arikawa, Y. Murakami and Y. Takasu, *J. Appl. Electrochem.* **28** (1998) 511.
25. N.V. Zhinkin, E.A. Novikov, N.S. Fedotova, V.I. Éberil' and V.B. Busse-Macukas, *Élektrokhimiya* **25** (1989) 1094.

26. A.A. Uzbekov and V.S. Klement'eva, *Élektrokhimiya* **21** (1985) 758.
27. L.A. De Faría, J.F.C. Boodts and S. Trasatti, *Electrochim. Acta* **42** (1997) 3525.
28. M.D. Spasojević, N.V. Krstajić and M.M. Jakšić, *J. Res. Inst. Catalysis*, *Hokkaido Univ*. **31** (1983) 77; **32** (1984) 19.
29. F. Hine, M. Yasuda, T. Noda, T. Yoshida and J. Okuda, *J. Electrochem. Soc*. **126** (1979) 1439.
30. R.G. Érenburg, L.I. Krishtalik and N.P. Rogozhina, *Élektrokhimiya* **20** (1984) 1183.
31. L.I. Krishtalik, *Electrochim. Acta* **26** (1981) 329.
32. D.A. Denton, J.A. Harrison and R.I. Knowles, *Electrochim. Acta* **24** (1979) 521.
33. M.R. Gennero de Chialvo and A.C. Chialvo, *Electrochim. Acta* **44** (1998) 841.
34. L.D. Burke, O.J. Murphy, J.F. O'Neill and S. Venkatesan, *J. Chem. Soc. Faraday Trans. I* **73** (1977) 1659.
35. F.I. Mattos-Costa, P. de Lima-Neto, S.A.S. Machado and L.A. Avaca, *Electrochim. Acta* **44** (1998) 1515.
36. K.W. Kim, E.H. Lee, J.S. Kim, K.H. Shin and K.H. Kim, *Electrochim. Acta* **46** (2001) 915.
37. Ch. Comninellis and G.P. Vercesi, *J. Appl. Electrochem*. **21** (1991) 335.
38. L.A. da Silva, V.A. Alves, M.A.P. da Silva, S. Trasatti and J.F.C. Boodts, *Electrochim. Acta* **42** (1997) 271.
39. A.I. Onuchukwu and S. Trasatti, *J. Appl. Electrochem*. **21** (1991) 858.